catalysts

MDPI

Supplementary Materials

Photocatalytic Performances and Antifouling Efficacies of Alternative Marine Coatings Derived from Polymer/Metal Oxides (WO_3@TiO_2) -Based Composites

Sunida Thongjamroon, Jatuphorn Wootthikanokkhan * and Nuchthana Poolthong

Materials Technology Program, School of Energy, Environment and Materials,
King Mongkut's University of Technology Thonburi (KMUTT), 126 Pracha Uthit Rd., Bang Mod, Thung Khu, Bangkok 10140, Thailand; sunida.th@mail.kmutt.ac.th (S.T.); nuchthana.poo@kmutt.ac.th (N.P.)
* Correspondence: jatuphorn.woo@kmutt.ac.th; Tel.: +66-0-2470-8692; Fax: +66-0-2427-9843

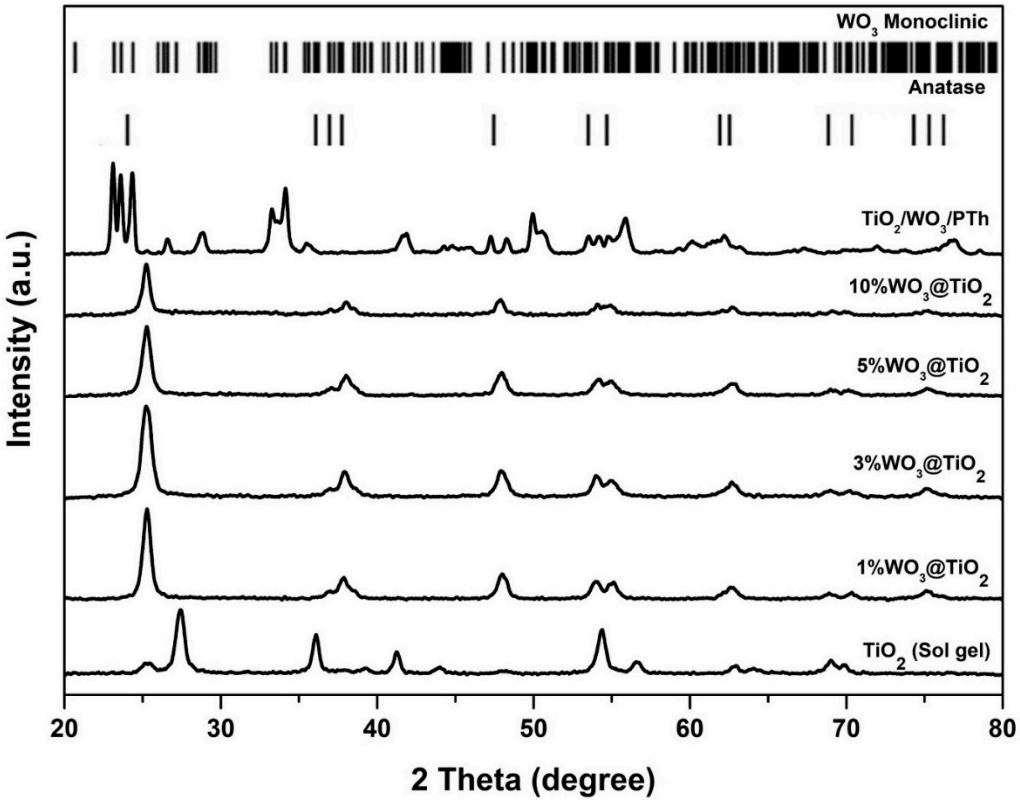

Figure S1. XRD patterns of the physically mixed metal oxides (TiO_2/WO_3) and the composite metal oxides (WO_3@TiO_2) synthesized by sol–gel process.

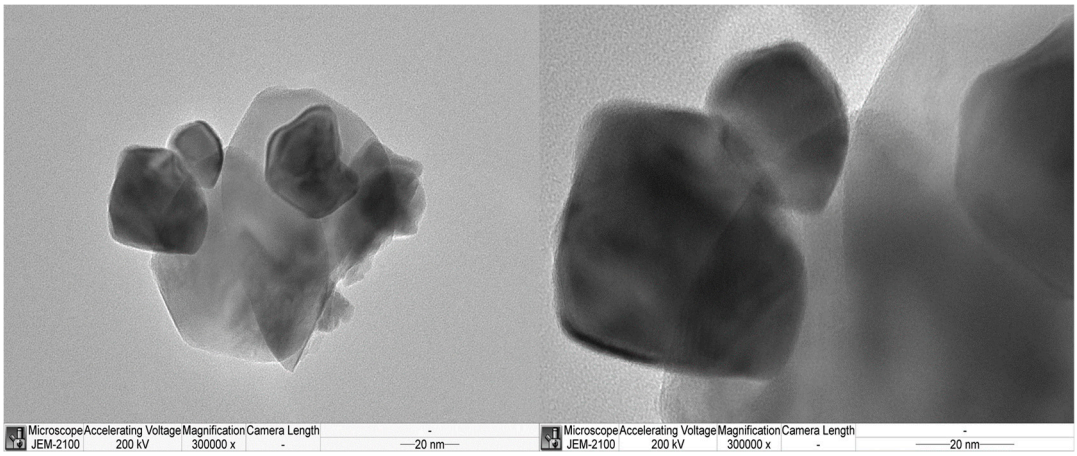

Figure S2. TEM image of the mixed metal oxide (TiO_2/PTh/WO_3).

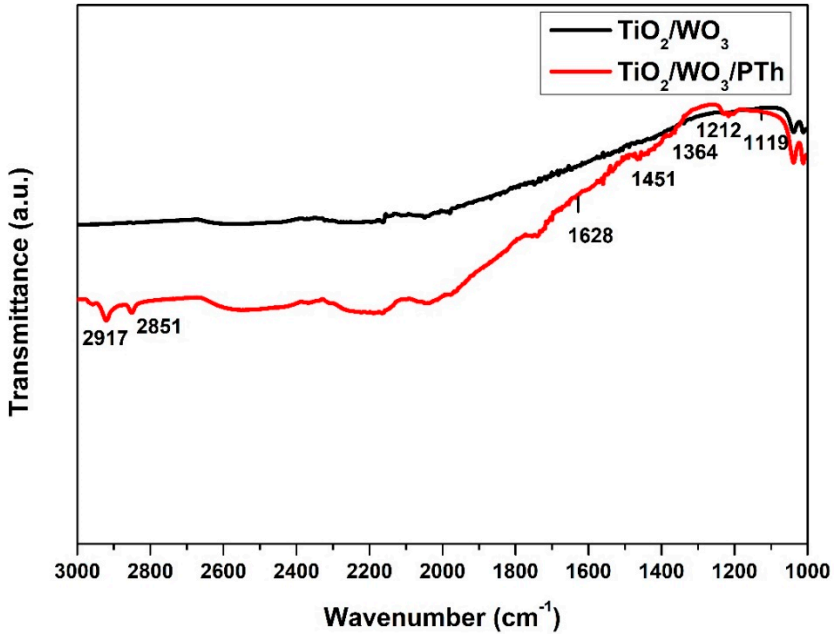

Figure S3. FTIR spectra of mixed metal oxides (**black**) TiO_2/WO_3, (**red**) TiO_2/PTh/WO_3; the peak at 1119 cm^{-1} was assigned to C–S–C bond vibration, the peak at 1212 cm^{-1} belongs to the C–O stretching bond, the peak at 1364 cm^{-1} was assigned to C–H, the peak at 1451 cm^{-1} is characteristic of aromatic C=C stretching vibration, the peak at 1628 cm^{-1} represents C=O symmetric stretching vibration modes of thiophene ring, the peak at 2166 cm^{-1} refers to C=C bond, and the peaks at 2851 and 2917 cm^{-1} are assigned to C–H stretching vibration.

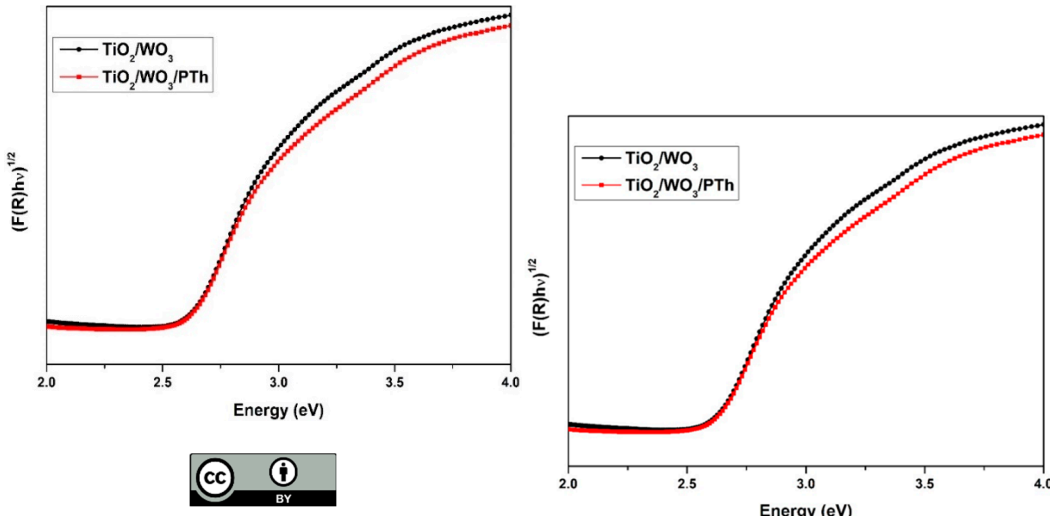

(a) (b)

Figure S4. UV/Vis spectra (**a**) and the transferred Kubelka–Munk vs. absorption energy plots (**b**) of the mixed metal oxides (TiO_2/WO_3 and $TiO_2/PTh/WO_3$).

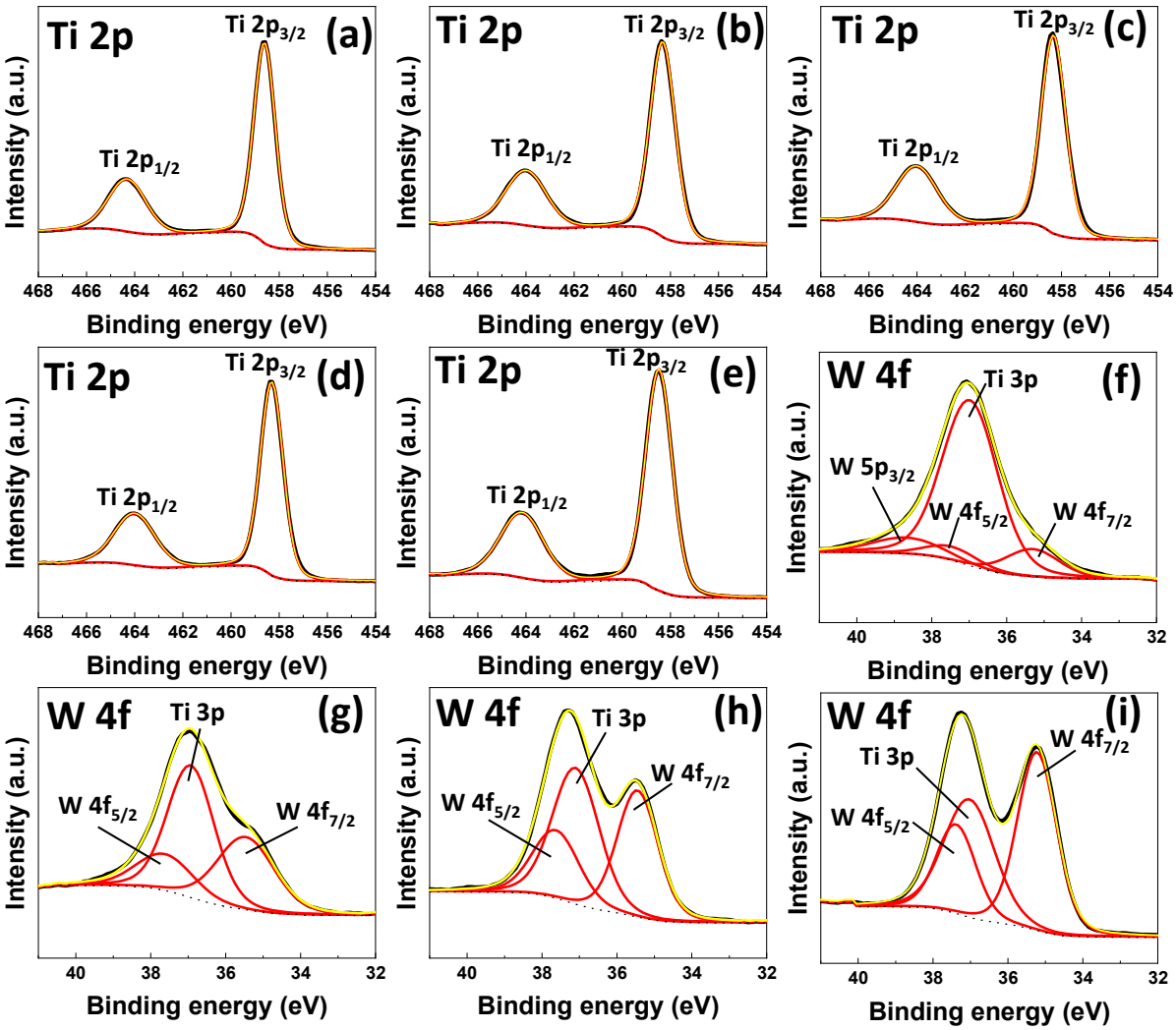

Figure S5. High-resolution XPS spectra of various metal oxides; images (**a**)–(**e**) present Ti 2p spectra of TiO_2 (**a**), 1%WO_3@TiO_2 (**b**), 3%WO_3@TiO_2 (**c**), 5%WO_3@TiO_2 (**d**), and 10%WO_3@TiO_2 (**e**), respectively. Images (**f**)–(**i**) present W 4f spectra of 1%WO_3@TiO_2 (**f**), 3%WO_3@TiO_2 (**g**), 5%WO_3@TiO_2 (**h**), and 10% WO_3@TiO_2 (**i**), respectively.

Part 2: A study on the effect of scavengers

Method

In this experiment, radical scavengers, such as silver (I) nitrate ($AgNO_3$), potassium iodide (KI), para-benzoquinone (*p*–BQ), and isopropanol (IPA), were used as radical scavengers of e^-, h^+, $O_2^{\bullet-}$, and $OH^\bullet$, respectively. The amount of catalyst (10%WO_3/TiO_2) and the initial concentration of MB were the same as used in the photocatalytic test except that the radical scavenger was dropwised into the MB solution (0.1 M in MB solution) before starting the experiment. Under the light condition, the solution was irradiated for 120 min and the concentration of MB left in solution was measured. For the dark condition, the solution was exposed to the light source for 1 min. Then, the light was turned off and the concentration of MB was collected at 30 min after that. The scavenging effect of the control experiment (blank) was also investigated.

Results and discussion

Possible reactive species occurred during photocatalytic reaction for methylene blue (MB) photodegradation-composed electron (e^-), hole (h^+), superoxide radical ($O_2^{\bullet-}$), and hydroxyl radical ($OH^\bullet$), and the possible reaction mechanism is illustrated in Equation 1 to 7 [52]. To investigate the species that dominantly involved the photocatalytic reaction MB and its charge transport mechanism, radical scavengers, such as silver (I) nitrate ($AgNO_3$), potassium iodide (KI), para-benzoquinone (*p*–BQ), and isopropanol (IPA), which were used as the radical scavengers of e^-, h^+, $O_2^{\bullet-}$, and $OH^\bullet$, respectively, were carried out [53,54]. As shown in Figure 6(b) of the main manuscript, addition of KI as h^+ scavenger has a negligible effect on photodegradation efficiency of MB when compared to the control experiment (blank test), while addition of $AgNO_3$ as e^- scavenger under the same concentration significantly suppressed photodegradation efficiency of catalyst. From this evidence, therefore, it can be concluded that e^- is an important species to control the photocatalytic performance of catalyst rather than h^+. Interestingly, from scavenger experiments of h^+, h^+ at the valence band of either TiO_2 or WO_3 of composite catalyst (10% WO_3/TiO_2) could not be utilized as an active species to react with H_2O and OH^- for promoting $OH^\bullet$ species, as shown in Equation 5 and 6.

Furthermore, it was also observed that adding an IPA, which was used as $OH^\bullet$ scavenger, largely lowered photocatalytic performance of the catalyst. This indicates that $OH^\bullet$ is the most predominant active species and has greater influence than e^-. Thus, the possible reactive species for producing $OH^\bullet$ is an e^-, which locates at the conduction band of TiO_2. This $OH^\bullet$ species effectively reacted with dissolved O_2 to produce $O_2^{\bullet-}$, as shown in Equation 2. This $O_2^{\bullet-}$ was then reacted with H^+ ions to produce $OH^\bullet$ (Equation 3). To further verify this assumption that the $O_2^{\bullet-}$ behaves as intermediate to form $OH^\bullet$, *p*–BQ was added into MB solution to scavenge $O_2^{\bullet-}$ generated by e^-. The result showed that the addition of *p*–BQ significantly suppressed MB degradation efficiency. This efficiency was comparable to adding IPA as $OH^\bullet$ scavenger (see also Figure 6b in the main manuscript). This suggests that the $O_2^{\bullet-}$ is an important intermediate to produce $OH^\bullet$, which is the most highly reactive species for degrading MB. Therefore, for 10% WO_3/TiO_2 system, e^-, $O_2^{\bullet-}$, and $OH^\bullet$ were the main reactive species. Interestingly, it was reported that the existence of oxygen vacancies on the surface of photocatalyst can effectively induce generation of $O_2^{\bullet-}$ radicals [55]. This is why the 10% WO_3/TiO_2 that composed highest amount of oxygen vacancy showed the highest photocatalytic efficacy among the other catalysts.

$$WO_3/TiO_2 + h\nu \rightarrow WO_3/TiO_2\ (e^-_{TiO_2,CB} + h^+_{WO_3,VB}) \quad (1)$$

$$O_2 + e^-_{TiO_2,CB} \rightarrow O_2^{\bullet -} \quad (2)$$

$$O_2^{\bullet -} + e^-_{TiO_2,CB} + 2H^+ \rightarrow OH^- + OH^\bullet \quad (3)$$

$$O_2 + 3e^-_{TiO_2,CB} + 2H^+ \rightarrow 2OH^- \quad (4)$$

$$H_2O + h^+_{WO_3,VB} \rightarrow OH^\bullet + H^+ \quad (5)$$

$$OH^- + h^+_{WO_3,VB} \rightarrow OH^\bullet \quad (6)$$

$$OH^\bullet + MB \rightarrow Product \quad (7)$$

According to results of the effect of various scavengers and the above discussion, there are two possible charge transportation mechanisms, including Type II heterojunction as a double charge transfer mechanism and Z−scheme mechanism. From the h^+ scavenging result, it can be concluded that the h^+ at the valence band of both TiO_2 and WO_3 did not produce $OH^\bullet$ during photocatalytic reaction. Thus, if the charge transport process of catalyst is according to the Type II heterojunction, the h^+ at the valence band of WO_3 will transfer to the valence band of TiO_2, performing oxidation reaction of water, while the photoexcited e^- at the conduction band of TiO_2 will migrate to the conduction band of WO_3, yielding the reduction reaction of the dissolved oxygen. However, among all prepared catalysts, the photocatalytic degradation of MB of 10%WO_3/TiO_2 was too high. Thus, the $OH^\bullet$ species was impossibly generated from e^- at the conduction band of WO_3, which had low loading content in TiO_2. In addition, due to the exceptional photocatalytic performance of 10%WO_3/TiO_2, it was expected that the charge transfer and charge separation efficiency of this composite catalyst were much higher than the charge transportation of Type II heterojunction. Therefore, the scavenging experiment revealed that e^-, $O_2^{\bullet -}$, and $OH^\bullet$ were the predominant active species; the transport process of charge carriers of the photogenerated $e^- - h^+$ pairs should not follow the common Type II heterojunction mechanism. Thus, the possible charge transfer mechanism of 10%WO_3/TiO_2 should be Z-scheme mechanism, which significantly possessed high charge transport and charge separation efficiency compared to Type II heterojunction. This charge transport type not only accelerates transport efficiency of photoexcited charges but can also preserve redox ability for efficient degradation of MB.

From the above discussion, the charge transport mechanism was proposed as Z-scheme, as shown in Figure 8 of the main manuscript. First, both TiO_2 and WO_3 could be easily excited by UV irradiation, leaving h^+ and e^- at the valence band and conduction band, respectively, as shown in Equation 1. Then, the e^- located in the conduction band of WO_3 transferred to the intimated valence band of TiO_2 through the interface of heterostructure between WO_3 and TiO_2, as shown in TEM image. This e^- derived from WO_3 would recombine with the photogenerated h^+ at the valence band of TiO_2. As a result, the e^- would be accumulated in the conduction band of TiO_2, which further reacted with dissolved O_2 to produce $O_2^{\bullet -}$ and $OH^\bullet$, while the h^+ would be retained in the valence band of WO_3 and further reacted with H_2O to produce $OH^\bullet$. Generation of $OH^\bullet$ as highly reactive species facilitated to degrade MB through oxidation reaction under the light condition (Equation 7). However, the WO_3 loading in the composite catalyst was low (see the result from EDX in Table 1 of the main manuscript). Thus, the amount of $OH^\bullet$ generated by h^+ in WO_3 was much lower than that produced by e^- from the conduction band of TiO_2.

For the charge transport mechanism in the dark condition of 10%WO_3/TiO_2, the scavenging experiment showed that the predominant reactive species were e^- and $OH^\bullet$, while h^+ had little effect on the catalytic performance when compared to the control experiment (blank), as shown in Figure 6(b) of the main manuscript. Thus, it can be concluded that the small amounts of photogenerated h^+ could react with H_2O to produce $OH^\bullet$ species. Thus, the Z-scheme charge transfer that was proposed for the light condition would convert into Type II heterojunction transport phenomenon, as demonstrated in Figure 8 (ii).

The possible reason is the band energy alignment between TiO_2 and WO_3, the tendency of charge transfer without driving force (photon), and the location of accumulated charges before turning off the light. Thus, under the dark condition, the Z-scheme mechanism is impossible to draw. After turning off the light, relaxation of photoexcited charges (e^- and h^+) to the lower energy as compared to their energy at the excited state automatically occurred. The e^- accumulated in the conduction band of TiO_2 would transfer back to the conduction band of WO_3, and some e^- at this conduction band might transfer and recombine with h^+ at the valence band of TiO_2. In addition, h^+ retained in the valence band of WO_3 would transport to the valence band of TiO_2 by proper alignment between the valence band of WO_3 and TiO_2. As a result, the $O_2^{\bullet-}$ and $OH^{\bullet}$ could be produced at the conduction band of WO_3 and the valence band edge of TiO_2, respectively. Therefore, catalytic degradation of MB could be performed in the dark condition using composite catalyst. The redox processes were carried on and saturated when the charge transfer reached equilibrium situation. Thus, it can be concluded that the charge transport mechanism of the prepared 10%WO_3/TiO_2 composite follows a solid-state Z-scheme and Type II heterojunction mechanisms under the light and dark conditions, respectively.

For the TiO_2/Pth/WO_3, the transport mechanism of the photogenerated charges was expected to be a Type II heterojunction, as shown in Figure 8 (iii) of the main manuscript. This is the normal mechanism that can be found for weak interaction WO_3/TiO_2 [40,56]. Although the charge transport efficiency of TiO_2/Pth/WO_3 was better than that of the physical mixing of WO_3 and TiO_2 without polythiophene as binder (WO_3/TiO_2), its photocatalytic efficiency was much lower than that of WO_3/TiO_2 synthesized by in situ sol–gel method. Thus, the quality of the interaction between WO_3 and TiO_2 interface can affect charge transport efficiency of photogenerated charges and also control type of charge transport mechanism.